

Polycaprolactone scaffold engineered for sustained release of resveratrol: therapeutic enhancement in bone tissue engineering

Manjunath Srinivas Kamath¹
Shiek SSJ Ahmed²
M Dhanasekaran³
S Winkins Santosh¹

¹Department of Biotechnology, School of Bioengineering, SRM University,

²Department of Biotechnology, Chettinad Hospital and Research Institute, ³Department of Stem Cells, Life Line Rigid Hospital Pvt Ltd, Kilpauk, Tamil Nadu, India

Abstract: Biomaterials-based three-dimensional scaffolds are being extensively investigated in bone tissue engineering. A potential scaffold should be osteoconductive, osteoinductive, and osteogenic for enhanced bone formation. In this study, a three-dimensional porous polycaprolactone (PCL) scaffold was engineered for prolonged release of resveratrol. Resveratrol-loaded albumin nanoparticles (RNP) were synthesized and entrapped into a PCL scaffold to form PCL-RNP by a solvent casting and leaching method. An X-ray diffraction study of RNP and PCL-RNP showed that resveratrol underwent amorphization, which is highly desired in drug delivery. Furthermore, Fourier transform infrared spectroscopy indicates that resveratrol was not chemically modified during the entrapment process. Release of resveratrol from PCL-RNP was sustained, with a cumulative release of 64% at the end of day 12. The scaffold was evaluated for its bone-forming potential in vitro using human bone marrow-derived mesenchymal stem cells for 16 days. Alkaline phosphatase activity assayed on days 8 and 12 showed a significant increase in activity (1.6-fold and 1.4-fold, respectively) induced by PCL-RNP compared with the PCL scaffold (the positive control). Moreover, von Kossa staining for calcium deposits on day 16 showed increased mineralization in PCL-RNP. These results suggest PCL-RNP significantly improves mineralization due to its controlled and prolonged release of resveratrol, thereby increasing the therapeutic potential in bone tissue engineering.

Keywords: therapeutic scaffolds, polycaprolactone scaffolds, bone tissue engineering, resveratrol, albumin nanoparticles, mesenchymal stem cells

Introduction

Regeneration of closed and compound fractures of bone tissue with bone loss of more than 3 cm is a complex process. In comminuted and segmental fractures having bone loss of more than 6 cm, the chances of deformity, shortening of bones, and recurrent fractures due to nonunion, malunion, or cross-union after healing are common.¹⁻³ Treatment for bone fractures measuring more than 3 cm includes autograft, allograft, xenograft, and transplant with permanent synthetic materials.¹ Autologous transplantation of a bone graft from the iliac crest is considered the “gold standard” for treatment of complex fractures.⁴ However, such traumatic harvesting of bones is associated with risks of morbidity due to nerve injury, causing numbness, difficulty in walking, decreased sexual activity, and persistent back pain.⁵ Allografts and xenografts have proven to be inferior to autografts and are associated with risks of graft rejection, disease transmission, and nonunion of grafts at the fracture site,^{1,4} whereas transplant of permanent synthetic materials induces osteolysis and an inflammatory response. To overcome the complexity of bone loss and morbidity, three-dimensional scaffolds

Correspondence: S Winkins Santosh
Department of Biotechnology,
School of Bioengineering,
SRM University, Kattankulathur
603 203, Tamil Nadu, India
Tel +91 86 9522 2205
Email regenmed79@gmail.com

made of biomaterials are being extensively studied. Three-dimensional scaffolds can increase orientation of cells and provide solid support for cells in the margin of fractured bone to attach and grow into the fractured space, thereby decreasing the risk of malunion or cross-union. Also, three-dimensional scaffolds fortified with nanohydroxyapatite and bioglass ceramics increase mechanical strength, in addition to having osteoconductive properties,⁶ whereas metallic nanoparticles, such as silver, zinc, and copper, increase the antimicrobial activity of these scaffolds.⁷ Further, the scaffolds should also possess properties to enhance cell attachment and proliferation, to facilitate angiogenesis, and to increase calcium deposition when inserted into the fractured site.⁶ In brief, treatment of complex bone fractures with three-dimensional scaffolds is promising, provided that scaffolds are osteoconductive and osteoinductive, and are able to facilitate osteogenesis.

Clinically, sustained release of recombinant human bone morphogenic protein-2 for bone formation revealed severe complications, including swelling in the throat and neck, radiculitis, obstruction of the airways due to local swelling, swelling in the tissues and organs surrounding the site of release of recombinant human bone morphogenic protein-2, and an increased incidence of cancer and male sterility.^{8–11} Since factors like bone morphogenic proteins, basic fibroblast growth factor, and transforming growth factor beta are a class of indigenous growth factors which signal numerous pathways in the human system, release of these factors at a therapeutic site could produce undesirable side effects in surrounding tissues, apart from bone regeneration. Also due to continuous release of these factors, they could be absorbed into the blood stream and produce systemic effects. Therefore, therapeutic use of indigenous growth factors for a prolonged time is not desirable. Ideally, a bioactive molecule used for therapeutic enhancement in tissue engineering should not cause any undesirable effects in the human system. Bioactive small molecules of plant origin with the potential to induce osteogenesis and not eliciting any unfavorable events in the human system could be released at the site of bone regeneration.

Resveratrol is a polyphenolic phytoestrogenic compound obtained from plants. It has been extensively studied for its anticancer activity, antiaging activity, and potential antioxidant properties, apart from its osteogenic potential. Resveratrol is widely used as an antioxidant supplement, and its long-term use has not been reported to have adverse effects on the human system. Hence, therapeutic targeting of resveratrol in micromolar concentrations is safe and effective

for bone tissue engineering. Sustained release of resveratrol by entrapping resveratrol-loaded albumin nanoparticles (RNP) into scaffolds increases the therapeutic potential of the scaffold in bone tissue engineering. A previous study reported that sustained release of resveratrol from nanofibers increases alkaline phosphatase and calcium deposits *in vitro*.¹² In brief, treatment of complex bone fractures with three-dimensional scaffolds is promising, provided scaffolds are osteoconductive and osteoinductive, and are able to facilitate osteogenesis.

Resveratrol is a well studied polyphenolic phytoestrogen that promotes proliferation and differentiation of bone marrow-derived mesenchymal stem cells into osteoblasts.⁸ Resveratrol increases alkaline phosphate activity, enhancing differentiation of bone marrow-derived mesenchymal stem cells to an osteoblast lineage.^{12–14} Resveratrol also increases proliferation and differentiation of osteoblasts, thus increasing the propensity for bone formation.¹⁵ Although resveratrol has the potential to enhance bone formation, it is rapidly metabolized and excreted from the body as sulfated and monoglucuronide derivatives.^{16,17} Controlled release of resveratrol at the site of bone loss could be more efficient than oral administration. Hence a three-dimensional porous polycaprolactone (PCL) scaffold was fortified with RNP to release resveratrol in a controlled manner, thereby overcoming the effects of rapid resveratrol clearance from the body. PCL is a synthetic polymer that has been widely investigated in tissue engineering and drug targeting. The bioabsorbability, biocompatibility, and mechanical strength of PCL makes it well suited for bone tissue engineering.¹²

Bone regeneration could be accelerated by supplementing scaffolds with bioactive molecules that increase proliferation and differentiation of mesenchymal stem cells into osteoblasts and promote osteoblast proliferation and calcium deposition. Based on this hypothesis, we developed PCL-RNP and evaluated its bone-forming potential and drug release kinetics *in vitro*. Morphologic analyses of PCL-RNP scaffolds were done by scanning electron microscopy and qualitative analysis by Fourier transform infrared (FTIR) spectroscopy and X-ray diffraction. Further, physical characterization of RNP was carried out using scanning electron microscopy, atomic force microscopy, and a zetasizer. The mineralization potential of PCL-RNP was evaluated *in vitro* using human bone marrow-derived mesenchymal stem cells (hBMSCs) wherein an alkaline phosphatase assay showed increased activity in PCL-RNP compared with a PCL scaffold (the positive control). Moreover, PCL-RNP potentially increased

mineralization compared with PCL (negative and positive controls), which was confirmed with von Kossa staining for calcium deposition. The results obtained suggest enhancement of the therapeutic potential of PCL-RNP *in vitro* as a result of sustained and prolonged release of resveratrol.

Materials and methods

Bone marrow cells were harvested in accordance with ethics committee requirements by obtaining written informed consent from patients undergoing experimental cell therapy for spinal injury. The protocol for sample collection was reviewed and accepted by the ethics committee of Life Line Rigid Hospital, Chennai, India.

Preparation of RNPs

RNPs were prepared by a coacervation process described elsewhere.¹⁸ Briefly, albumin (2% w/v) was dissolved in deionized water and the pH was adjusted to 7. Resveratrol 10 mg was dissolved in 200 μ L of ethanol and added dropwise to the albumin solution and incubated for one hour in the dark at room temperature. Ethanol was added dropwise at a flow rate of 1 mL per minute under constant stirring until the solution became turbid. Next, 8% glutaraldehyde was added to harden the coacervates. The mixture was stirred constantly for 2 hours to crosslink the proteins. The nanoparticles formed were centrifuged at 18,000 rpm and 4°C for 30 minutes. The supernatant was stored for estimation of unbound resveratrol. The pellet was suspended in phosphate-buffered saline (pH 7.4), centrifuged at 18,000 rpm and 4°C for 30 minutes, resuspended in phosphate-buffered saline, and lyophilized. The entrapment efficiency (E) of the process was calculated using the formula

$$E = [(T_{\text{Res}} - F_{\text{Res}})/T_{\text{Res}}] \times 100\%$$

where T_{Res} is the total amount of resveratrol added and F_{Res} is the free drug in the supernatant.

Preparation of scaffolds

PCL (molecular weight 80,000, purchased from Sigma-Aldrich, Bangalore, India) scaffold was prepared by a surface leaching method.¹⁹ Polycaprolactone (10% w/v) was dissolved in an equal solvent mixture of dichloromethane and ethanol followed by addition of RNP (10% w/w) to form PCL-RNP under constant stirring for 30 minutes. The mixture was then sonicated for 5 minutes on ice, and finely ground sucrose (particle size 100–200 μ m) was added in a ratio of 1:5 (PCL to sucrose), stirred to create a uniform slurry, and cast into

glass molds. These plates were dried at room temperature followed by leaching of sucrose from the scaffold in deionized water to form a porous structure. The porous scaffold was treated with 0.5 M NaOH for 4 hours to impart hydrophilicity and washed thoroughly with ethanol and phosphate-buffered saline under sterile conditions until the pH of the scaffold became neutral. PCL scaffolds prepared as described earlier without addition of RNP served as the control.

Characterization of materials

Scanning electron microscopy

The scaffolds were characterized by field emission scanning electron microscopy under low vacuum mode (60 Pa) with a low field detector and an applied voltage of 5 kV. The scaffolds were cut using a sharp razor to 1 cm \times 1 cm dimensions and placed on aluminum foil for scanning.

FTIR

The synthesized scaffolds were examined by FTIR using an Alpha FTIR spectrophotometer (Bruker Optics, Mumbai, India). First, 3 mg of the sample was mixed with 300 mg of potassium bromide (KBr) and made into pellet under vacuum. The pellet was then analyzed in the range of 4,000–500 cm^{-1} with a resolution of 1 cm^{-1} .

X-ray diffraction

The powdered scaffold was subjected to X-ray diffraction using the X'Pert-PRO (PANalytical, Almelo, The Netherlands) which operates at 40 kV with a current of 30 mA and uses $\text{K}\alpha$ radiation (1.544 Å). The 2 θ scan range was fixed at 5°–80° with a step angle of 0.0170.

Characterization of RNPs

Atomic force microscopy was performed using a 1500 scanning probe microscope (Agilent Technologies, Santa Barbara, CA, USA). A suspension containing the nanoparticles was diluted 1:100 times in water and coated on silicon tape in a spin coat unit under vacuum. Scanning of the particles was carried out in noncontact (ACAFM) mode with a scan speed of 3.007 lines per second; the cantilever force and frequency were 4% and 310.6 kHz, respectively.

Particle size, polydispersity index, and zeta potential were measured using a Mastersizer (Malvern Instruments, Malvern, UK). The average particle size was less than 200 nm and the polydispersity index was below 0.2, both of which were considered to be good, and the zeta potential was around ± 30 mV and also considered to be acceptable.

Analysis of resveratrol release from scaffolds

Prewritegged 1.5×1.5 cm scaffolds were incubated in 2 mL of phosphate-buffered saline under static conditions. At pre-determined time intervals, 300 μ L was removed by replacing equal amounts of phosphate-buffered saline. The absorbance of resveratrol released was read at 303 nm using an enzyme-linked immunosorbent assay reader. The concentration of resveratrol released was then obtained from the standard curve for resveratrol. The percentage release was calculated from the initial amount of nanoparticles entrapped per scaffold.

Collection of human bone marrow

A bone marrow sample (20 mL) was aspirated from the iliac crest region of three subjects aged 35–45 years and having a mean body mass index of 24.7 ± 2.6 kg/m². All samples were immediately processed to separate hBMSCs from the aspirated marrow.

Isolation and culture of hBMSCs

Mononuclear cells were obtained by density gradient centrifugation of bone marrow aspirates using Ficoll-Paque™ (GE Healthcare Life Sciences, Piscataway, NJ, USA).²⁰ The mononuclear cell layer was carefully aspirated and transferred to a tube containing 0.7% ammonium chloride solution and incubated at room temperature for 5 minutes to lyse any residual red blood cells. The cells were centrifuged at 450 rpm and 20°C for 10 minutes, the pellet was suspended in phosphate-buffered saline, and viability of the cells was determined using trypan blue exclusion staining. Further, cells were seeded at a density of 3.5×10^4 /cm² and cultured in Dulbecco's Minimum Essential Medium-Low Glucose (DMEM-LG, Invitrogen, Bangalore, India) supplemented with 10% fetal bovine serum (Invitrogen) and 1% antibiotic-antimycotic solution (Invitrogen) under standard culture conditions. The medium was changed once every 3 days until confluent (70%–80%) adherent cells were obtained. The primary hBMSC culture was subcultured for three passages with a change of medium twice a week. Further studies were carried out with the cells obtained after third passage.

Flow cytometric characterization of hBMSCs

Approximately 1×10^6 cells were treated with fluorochrome-tagged antibodies CD90-PERCP, CD44-FITC, CD29-PE, CD73-PE (BD Biosciences, Gurgoan, India), and CD105-APC (e Biosciences, Santiago, CA, USA), positive markers

for mesenchymal stem cells, CD34-PE (e Biosciences) and CD45-APC-Cy7 (e Biosciences), CD133-APC-A, CD31-FITC, HLA-DR-PERCP (BD Biosciences, India) negative markers. The cells were incubated with antibodies for 20 minutes in the dark and washed three times with wash flow buffer (phosphate-buffered saline supplemented with 2% [v/v] fetal bovine serum and 0.1% [w/v] sodium azide). Further, analyses were carried out using a FACS Aria™ flow cytometer (BD Biosciences) and data acquisition was done using FACSDiva™ software (BD Biosciences).²⁰

Multilineage differentiation potential of hBMSCs

Cells with 70%–80% confluency were harvested with trypsin 0.25%, and approximately 3×10^4 cells were cultured in DMEM-LG under standard conditions until 80% confluency.²⁰ The subconfluent cells were treated with osteogenic medium (DMEM-LG containing 10% fetal bovine serum, 1% antibiotic, 0.1 μ M dexamethasone, Sigma-Aldrich, India), 10 mM glycerophosphate (Sigma-Aldrich, India), and 2 mM ascorbic acid (Sigma-Aldrich, India) and cultured for 15 days. The culture was washed with phosphate-buffered saline (pH 7.4) and fixed with formalin (10%). von Kossa staining was performed to confirm calcium deposits. Silver nitrate 1% was added to the fixed cell culture and illuminated under ultraviolet light for 45 minutes. Sodium thiosulfate 5% was added, and the cell culture was then washed with distilled water for imaging under light microscopy.

Adipogenic differentiation was induced by addition of adipogenic medium to subconfluent culture.²⁰ The adipogenic medium contained DMEM-LG, 10% fetal bovine serum, 1% antibiotic-antimycotic solution, 0.1 μ M dexamethasone (Sigma-Aldrich), 0.5 mM isobutyl methylxanthine (Sigma-Aldrich), 1 μ g insulin (Sigma-Aldrich), and 200 mM indomethacin (Sigma-Aldrich). Cells were cultured in adipogenic medium for 14 days and fixed with 10% formalin in saline. The fixed cells were washed with 60% isopropanol and stained with Oil Red O (Sigma-Aldrich) for 10 minutes. The stained cells were then washed and imaged under light microscopy.

hBMSC seeding on scaffolds

hBMSCs were seeded onto sterile 1.5×1.5 cm scaffolds.²¹ Four different groups of scaffolds were seeded with cells at a density of 5×10^5 cells/mL and cultured under standard conditions. The groups were PCL-RNP, PCL-Res (10^{-6} M resveratrol added to medium), and PCL (positive control) cultured in osteogenic medium, and PCL (negative control)

cultured in DMEM-LG. The medium was supplemented with 10% fetal bovine serum and 1% antibiotic-antimycotic solution. After 6 hours of cell seeding, the scaffolds were transferred to fresh culture plates to negate the effect of cells voided from the scaffolds. The culture was carried out for 16 days with a change of medium every 3 days.

MTT assay for cytotoxicity

The MTT (3(4,5dimethylthiazol-eyl) 2,5diphenyl-tetrazoliumbromide, Sigma-Aldrich) assay was performed to evaluate cell viability.^{21,22} First, 1×10^3 cells were seeded onto the scaffolds (in the groups described above) and cultured under standard conditions. On day 7, the scaffolds were washed with phosphate-buffered saline and 100 μ L of MTT (5 mg/mL in sterile distilled water) was added and cultured for 10 hours. The formazan crystals formed were solubilized in dimethyl sulfoxide and read at 590 nm using an enzyme-linked immunosorbent assay reader.

Alkaline phosphatase assay

The cell-seeded scaffolds were washed with phosphate-buffered saline and alkaline phosphatase activity was assayed on days 8 and 12 using 5-bromo-4-chloro-3-indolyl phosphate/nitro blue tetrazolium (BCIP-NBT, Sigma-Aldrich).^{21,22} BCIP-NBT solution was prepared according to the manufacturer's protocol. Next, 200 μ L of BCIP-NBT was added to each scaffold and incubated for 2 hours. The violet crystals formed were solubilized with 300 μ L of sodium dodecyl sulfate 10% HCl solution for 18 hours. Absorbance was measured using the enzyme-linked immunosorbent assay reader at 595 nm.

von Kossa staining of mineralized scaffolds

On day 16, the cell-seeded scaffolds were washed with phosphate-buffered saline (pH 7.4) and fixed in 10% neutral buffered formalin.²⁰ The fixed scaffolds were cut horizontally with a uniform thickness of 10 μ m. The slides were flooded with 1% silver nitrate solution and incubated under an ultra-violet lamp for 45 minutes. Sodium thiosulfate 5% was added to stop the reaction, and the slides were thoroughly washed with tap water and imaged using light microscopy.

Statistical analysis

The data were imported into GeneSpring GX7.3 microarray software (Agilent Technologies) in which analysis of variance was carried out to determine the significant difference ($P \leq 0.05$) between PCL-RNP and other groups on alkaline

phosphatase and MTT assays.²³ All tests were performed using three different patient samples ($n = 3$) in triplicate.

Results and discussion

Material characterization

Scanning electron microscopy

Scanning electron microscopy of PCL-RNP showed highly interconnected porous structures with nanoparticles embedded on the surface of the scaffolds (Figure 1). The nanoparticles were uniformly spread throughout the surface, with few found to be agglomerated. The pore size of PCL-RNP was in the range of 50–150 μ m. Pore size and interconnectivity is an important factor for penetration of cells into scaffolds. Previous studies have shown that scaffolds with a pore size greater than 100 μ m are most suitable for cell penetration.²⁴ These observations suggest that these scaffolds are morphologically suitable for cell penetration.

FTIR analysis

The scaffolds were analyzed by FTIR spectroscopy. The measured transmittance of PCL-RNP (Figure 2D) showed

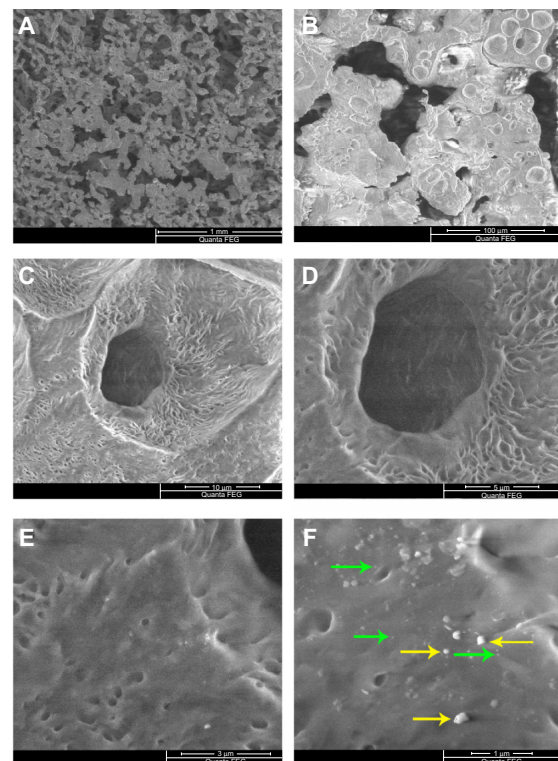


Figure 1 Scanning electron microscopy images of PCL-RNP. (A) PCL-RNP showing pores in the range of 50–100 μ m. (B–D) Further magnification into the scaffold. (E and F) Nanoparticles and agglomerates embedded on the surface of the scaffold.

Note: Green and yellow arrows show embedded nanoparticles and agglomerations, respectively.

Abbreviations: PCL, polycaprolactone; RNP, resveratrol-loaded albumin nanoparticles.

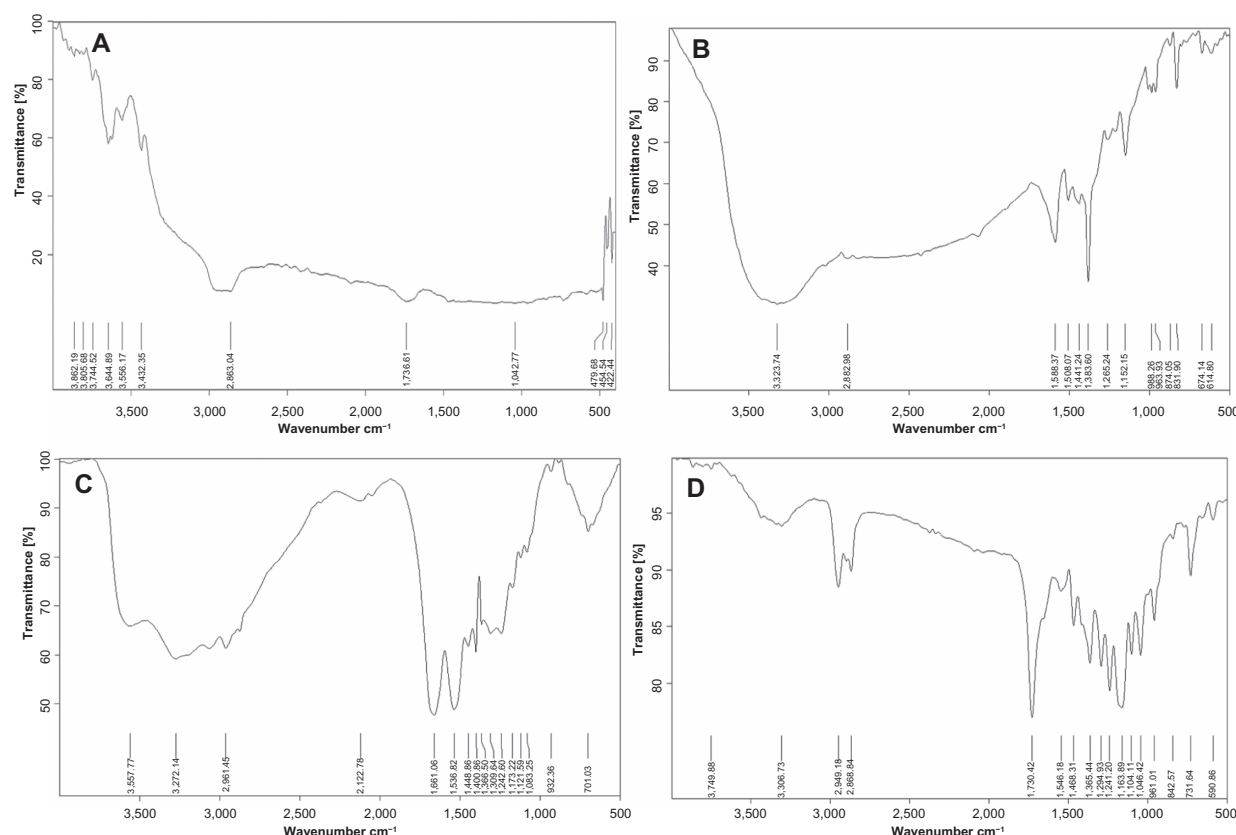


Figure 2 Fourier transform infrared spectra. (A) PCL spectra showing transmittance peaks for standard PCL. (B) Standard resveratrol spectra showing a typical trans olefinic band at $930\text{--}961\text{ cm}^{-1}$. (C) RNP spectra depicting albumin and characteristic resveratrol bands. (D) Standard PCL-RNP spectra show bands characteristic for PCL ($2,900\text{--}2,800\text{ cm}^{-1}$), resveratrol ($930\text{--}961\text{ cm}^{-1}$), and albumin.

Abbreviations: PCL, polycaprolactone; RNP, resveratrol-loaded albumin nanoparticles.

a strong band at $1,730\text{ cm}^{-1}$, corresponding to $\text{C}=\text{O}$ stretching, and two bands at $2,949.18\text{ cm}^{-1}$ and $2,868.84\text{ cm}^{-1}$, representing symmetric and asymmetric CH_2 bond stretching, respectively. These bands correspond to the aliphatic polyester PCL spectrum (Figure 2A).²⁵ Further, bands for albumin were observed in the range of $4,000\text{ cm}^{-1}$ to $1,500\text{ cm}^{-1}$.²² Absorption at $1,600\text{ cm}^{-1}$ to $1,450\text{ cm}^{-1}$ suggested an aromatic ring, and a band near $3,400\text{ cm}^{-1}$ to $3,300\text{ cm}^{-1}$ indicated an O-H group. A typical trans olefinic band was observed at 961.01 cm^{-1} (Figure 2B), which is a characteristic band for resveratrol.²⁵ There was no change in the bands for resveratrol in PCL-RNP, indicating that no chemical bonding between resveratrol, albumin, and PCL had occurred during synthesis and processing of the scaffolds. The RNP (Figure 2C) also showed the characteristic bands of resveratrol and albumin at corresponding wavelengths, as discussed above. Hence, resveratrol was not modified on initial entrapment into albumin nanoparticles. Our results show that resveratrol was not chemically altered and hence increases the potential of PCL-RNP in releasing resveratrol at the therapeutic site.

X-ray diffraction analysis

X-ray diffraction analysis was carried out to determine the crystallinity of PCL-RNP. Two semicrystalline peaks at a 2θ value of 21.6 and 23.8 were obtained for PCL-RNP (Figure 3).²⁵ Standard resveratrol showed peaks at 2θ values of 6.6 , 16.4 , 19.2 , 22.4 , 23.6 , 25.3 , and 28.4 .²⁵ However, no such peaks were seen for PCL-RNP and RNP, implying that resveratrol is amorphized during nanoencapsulation. The amorphization of resveratrol was due to loss of the structural arrangement of the lattice during its entrapment into RNP and consequently in PCL-RNP. The presence of resveratrol in PCL-RNP was confirmed by FTIR analysis and drug release studies. Hence, the absence of characteristic peaks of resveratrol is due to its amorphization. A previous study of microencapsulation of resveratrol²⁵ also reported amorphization and its importance in drug targeting. Amorphization in the solid state increases dissolution of a drug, which is preferred in drug targeting especially when the drug is hydrophobic. These results suggest entrapment of resveratrol in nanoparticle form into a scaffold improves the dissolution of resveratrol which, in

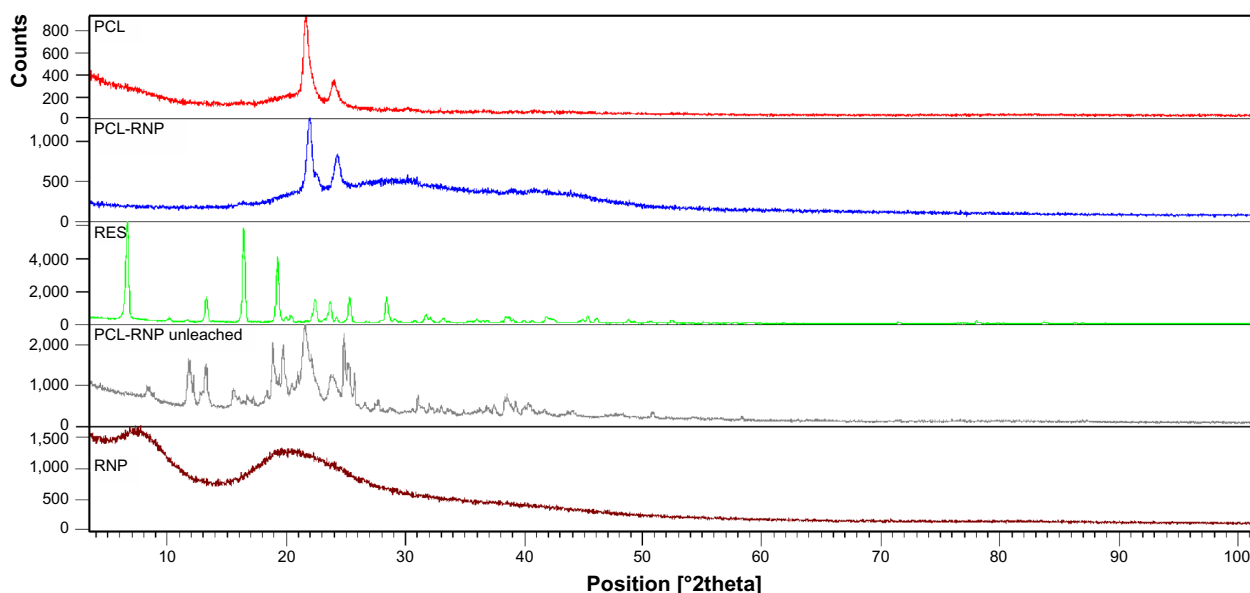


Figure 3 X-ray diffraction spectra of PCL, PCL-RNP, RNP, and resveratrol, confirming amorphization of resveratrol and crystalline nature of PCL in PCL-RNP. PCL-RNP unleached is the spectra of scaffolds before leaching which implies an absence of sucrose in PCL-RNP after leaching.

Note: Spectra overlapped using X'Pert High score plus software.

Abbreviations: PCL, polycaprolactone; RNP, resveratrol-loaded albumin nanoparticles; RES, resveratrol.

turn, increases the drug delivery potential of PCL-RNP in bone tissue engineering.

Characterization of RNPs

The size of the RNP was determined using atomic force microscopy, scanning electron microscopy, and a zetasizer. Atomic force microscopy showed the mean size of the RNP to be 172 nm. Similarly, scanning electron microscopy of the nanoparticles suggested the particle size to be in the range of 90–190 nm (Figure 4). Further, the polydispersity index, zeta potential, and average size of the RNP was recorded by zetasizer to be 0.035, –27.5 mV, and 133 nm, respectively. The zeta potential and polydispersity index indicate that the particles did not undergo agglomeration. Finally, the drug loading efficiency, calculated from the free drug in the supernatant, was found to be 55%. These results confirm that the particle size of RNP is well within that nanometer range, and that they are highly stable and potent drug carriers.

Analysis of resveratrol release from PCL-RNP

The release of resveratrol from PCL-RNP did not show a burst effect as compared with RNP, which showed a burst effect at 6 hours (Figure 5). Sustained release of resveratrol from PCL-RNP was observed until 12 days, with the total amount of resveratrol released at the end of 12 days being 64%, whereas RNP showed release of more than 80% in

6 days and a cumulative release of 90% at the end of 12 days. This sustained release of resveratrol from PCL-RNP is attributed to the entrapment of RNP into PCL, which acts as a barrier for the release of resveratrol from nanoparticles. These results confirm that entrapment of RNP into PCL scaffolds delayed the release of resveratrol, which is desirable for therapeutic scaffolds.

Characterization of hBMSCs

At third passage, the percentages of cells expressing CD90, CD105, CD73, CD44, and CD29 (positive markers for mesenchymal stem cells) were 99.4, 99.7, 99.2, 98.8, and 99.1, respectively (Figure 6-I). The percentages of cells expressing CD34, CD45, CD133, CD31, and HLA-DR (negative markers for mesenchymal stem cells) were found to be 5.7, 3.4, 3.4, 0.8, and 17 respectively (Figure 6-II). The percentage of contaminating hematopoietic lineages was negligible; further, the cells were adherent and maintained a flattened elongated shape throughout the passages (Figure 7). These results suggest that the cells harvested at third passage were mesenchymal. The plasticity of the adherent mesenchymal stem cells was confirmed by osteogenic and adipogenic differentiation (Figure 7). Confirmation of osteogenic differentiation was done by staining calcium deposits with von Kossa stain which turned calcium black by day 21. Adipogenic differentiation was confirmed by Oil Red O staining (which stains lipid vacuoles red) on day 18. Mesenchymal stem cells

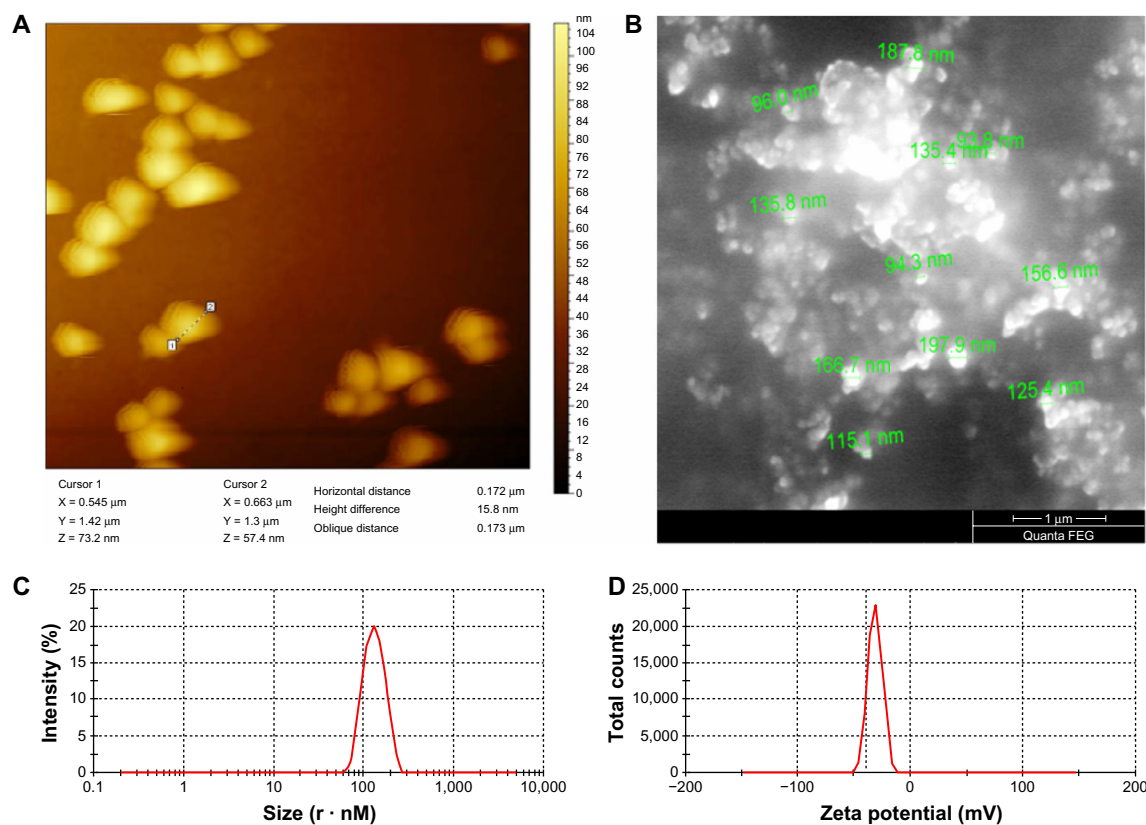


Figure 4 RNP characterization. (A) Atomic force microscopy image showing horizontal distance (particle diameter), (B) scanning electron microscopy shows particle sizes in the range of 90–190 nm, (C) polydispersity index of RNP, and (D) zeta potential spike of RNP.

Abbreviations: PCL, polycaprolactone; RNP, resveratrol-loaded albumin nanoparticles.

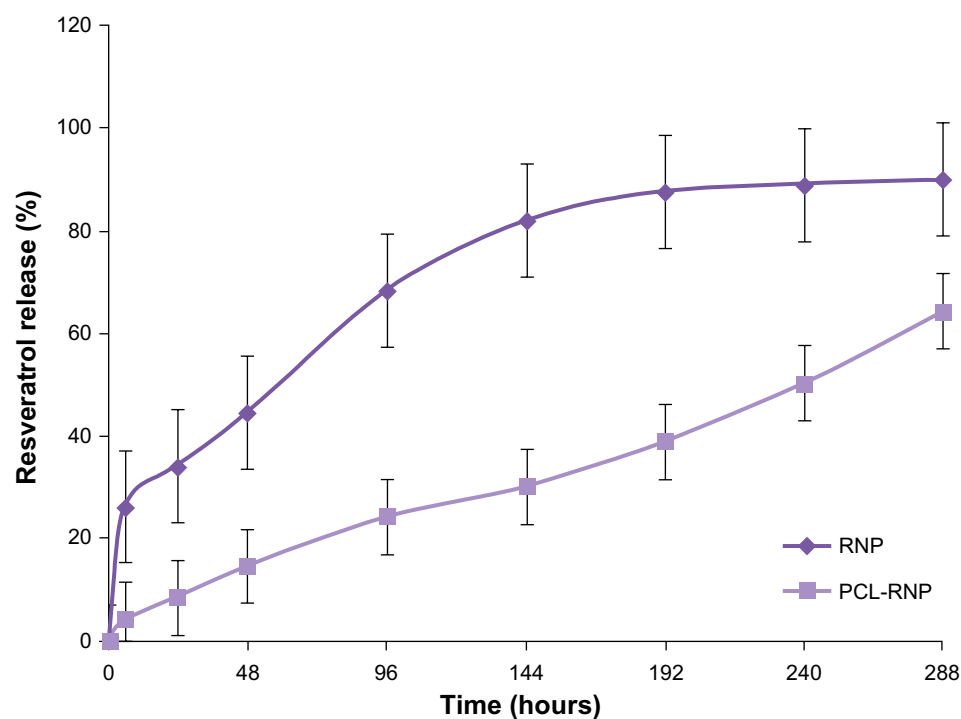


Figure 5 Comparative drug release profiles show that release of resveratrol was sustained until 288 hours in PCL-RNP without a burst effect. RNP shows a burst in release of resveratrol at hour 6.

Abbreviations: PCL, polycaprolactone; RNP, resveratrol-loaded albumin nanoparticles.

cultured in noninductive medium (DMEM-LG) served as the control for staining.

MTT and alkaline phosphatase assays

The MTT assay (Figure 8) showed that the scaffolds were not cytotoxic. A significant ($P \leq 0.01$) increase in activity was observed in PCL-RNP and PCL-Res compared with PCL (the positive control). This is due to the proliferative effect

of resveratrol on hBMSCs. A previous study also reported a dose-dependent proliferative effect of resveratrol.¹² In addition, the BCIP-NBT assay showed that alkaline phosphatase activity was significantly increased in PCL-RNP (Figure 9) compared with the positive control by 1.62-fold ($P \leq 0.001$) and 1.42-fold ($P \leq 0.001$) on day 8 and day 12, respectively. PCL-Res showed a significant increase of 1.6-fold ($P \leq 0.001$) and 1.4-fold ($P \leq 0.001$) on day 8 and

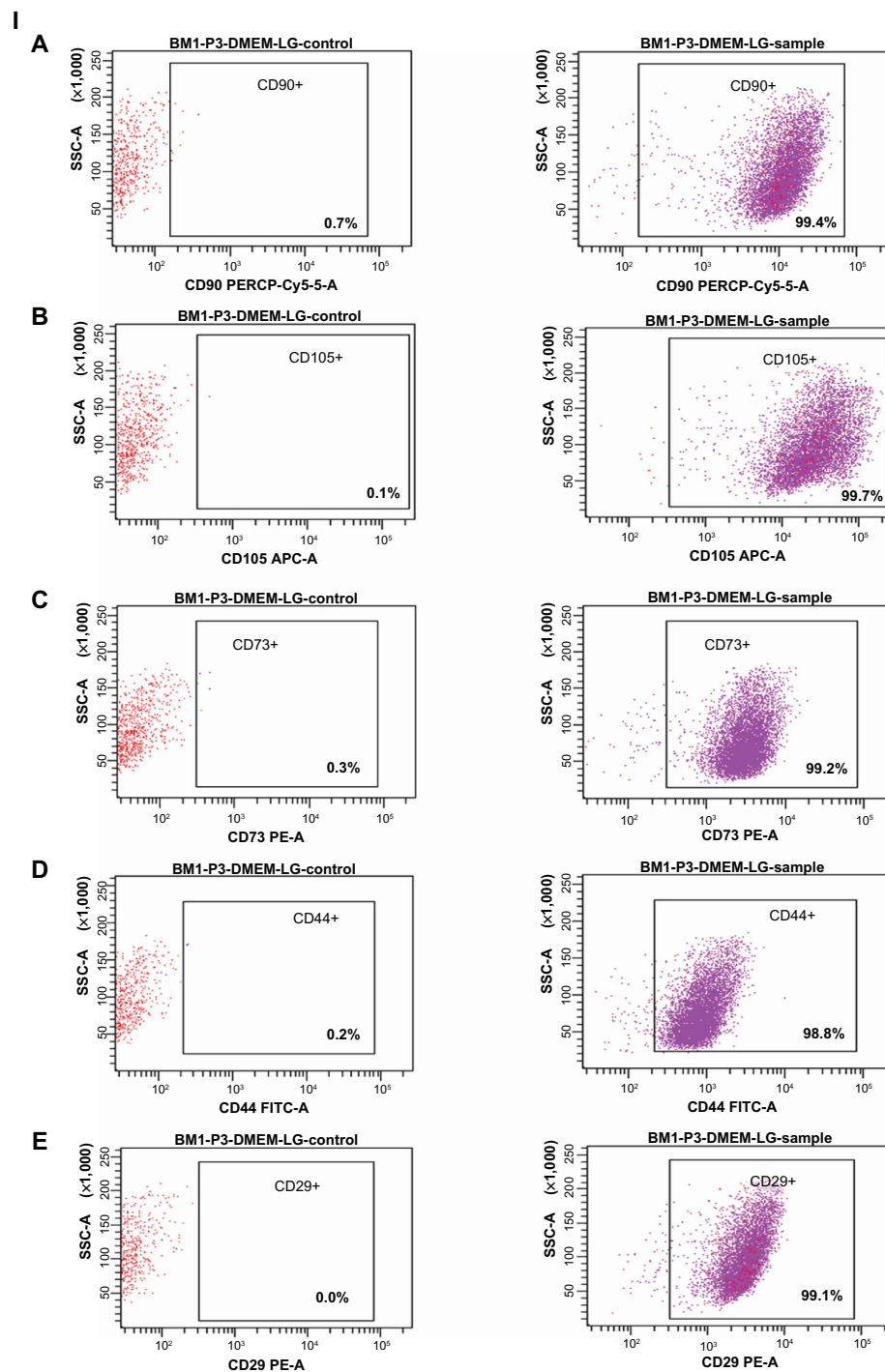


Figure 6 (Continued)

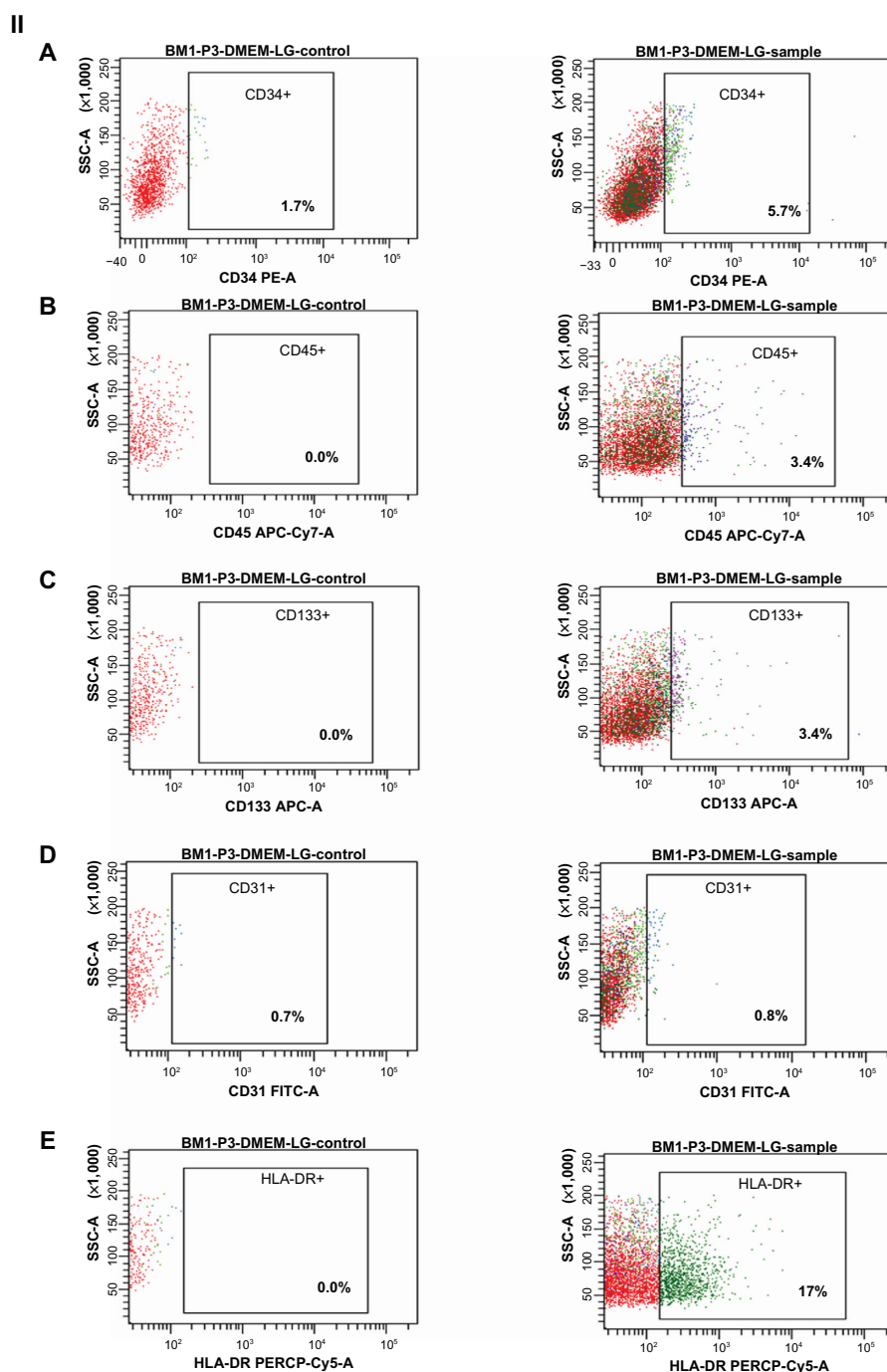


Figure 6 Immunophenotyping of cell surface markers of hBMSCs using flow cytometric analysis. (I) Positive markers for mesenchymal stem cells: (A) CD90-PERCP, (B) CD105-APC, (C) CD73-PE, (D) CD44-FITC, (E) CD29-PE, showing higher percentage expression (control and sample as labeled). (II) Negative markers for mesenchymal stem cells: (A) CD34-PE, (B) CD45-APC-Cy7, (C) CD133-APC-A, (D) CD31-FITC, (E) HLA-DR-PERCP show a low percentage expression (control and sample as labeled). **Note:** The surface marker profile shows that the cells obtained at third passage were mesenchymal stem cells. BM1-P3-DMEM-LG represents bone marrow cells obtained at third passage in DMEM-LG medium.

Abbreviations: DMEM-LG, Dulbecco's Minimum Essential Medium-Low Glucose; hBMSCs, human bone marrow-derived mesenchymal stem cells; SSC, side scatter; BM, bone marrow.

day 12, respectively, compared with the positive control. The results obtained imply that PCL-RNP was as potent as PCL-Res in inducing alkaline phosphatase activity. A previous study observed increased alkaline phosphatase activity over a wide range of concentrations (10^{-6} to 10^{-5} M)

of resveratrol.^{12–15} Hence, for a scaffold to be bioactive, the concentration of resveratrol release needs to be in the range of 10^{-11} M to 5 μ M.¹² Alkaline phosphatase is a key early marker in bone formation and differentiation of mesenchymal stem cells into an osteoblastic lineage. Hence, the increase in

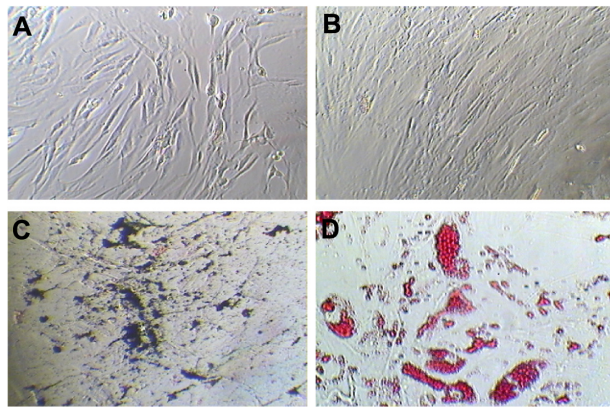


Figure 7 Characterization of hBMSCs at third passage. **(A)** Morphology of cells on day 7 of culture. **(B)** Morphology of hBMSCs on day 14, showing 80% confluency. **(C)** von Kossa staining for calcium deposits shown as black-colored crystals after osteogenic differentiation and **(D)** Oil O Red stains of lipids after adipogenic differentiation.

Note: All images were obtained under light microscopy at 100× magnification.
Abbreviation: hBMSCs, human bone marrow-derived mesenchymal stem cells.

alkaline phosphatase activity induced by PCL-RNP confirms that release of resveratrol is within the desired range, which further suggests that PCL-RNP is osteoinductive.

von Kossa staining of mineralized scaffolds

Calcium deposits in PCL-RNP, PCL-Res, and PCL (positive control) were compared and determined by von Kossa staining. The results showed increased calcium deposition in PCL-RNP and PCL-Res compared with the positive control (Figure 10). Further, the calcium deposits were present uniformly throughout the sections of PCL-RNP, PCL-Res, and the positive control. These results indicate the mineralizing and osteogenic properties of PCL-RNP. A previous report also suggested increased mineralization in nanofibers

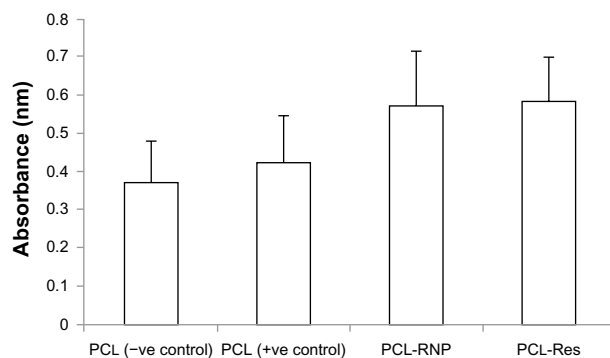


Figure 8 MTT assay on day 7 of cell seeding on scaffolds shows significantly increased activity of cells in PCL-RNP ($P \leq 0.01$) and PCL-Res ($P \leq 0.01$) compared with the positive and negative PCL controls.

Abbreviations: PCL, polycaprolactone; RNP, resveratrol-loaded albumin nanoparticles; Res, resveratrol.

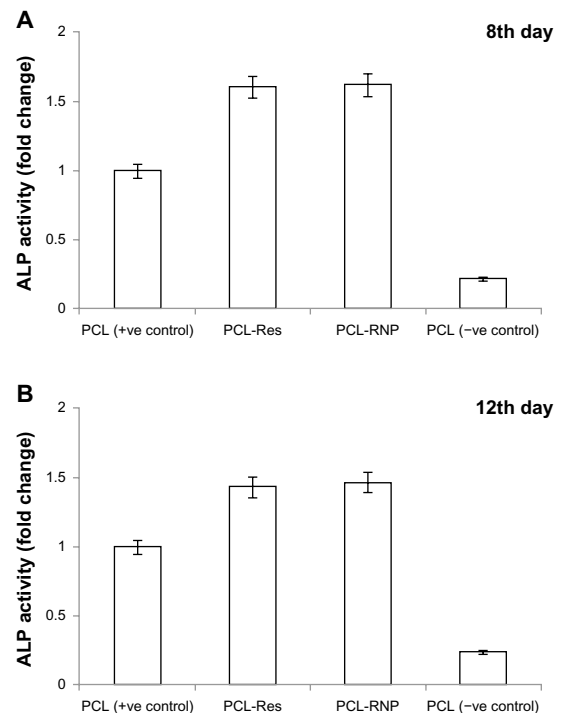


Figure 9 Alkaline phosphatase assay showing fold increase against PCL (positive control) activity taken as 100%. **(A)** Alkaline phosphatase assayed on day 8 shows significantly increased activity in PCL-RNP ($P \leq 0.001$) and PCL-Res ($P \leq 0.001$) compared with PCL (positive control) and **(B)** on day 12 of culture on scaffolds shows significantly increased activity in PCL-RNP ($P \leq 0.001$) and PCL-Res ($P \leq 0.001$) compared with PCL (positive control).

Note: Positive control, cell culture done on PCL scaffold in osteogenic medium; negative control, cell culture done on PCL scaffold in DMEM-LG medium.

Abbreviations: PCL, polycaprolactone; RNP, resveratrol-loaded albumin nanoparticles; Res, resveratrol; DMEM-LG, Dulbecco's Minimum Essential Medium-Low Glucose.

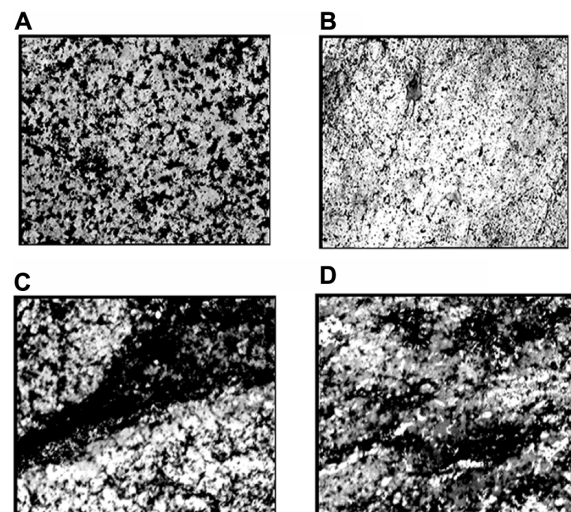


Figure 10 von Kossa stained scaffolds showing calcium deposits as black-colored patches with 250× magnification. **(A)** PCL (positive control), **(B)** PCL (negative control), **(C)** PCL-RNP, and **(D)** PCL-Res.

Note: Positive control, cell culture done on PCL scaffold in osteogenic medium; negative control, cell culture done on PCL scaffold in DMEM-LG medium.

Abbreviations: PCL, polycaprolactone; RNP, resveratrol-loaded albumin nanoparticles; Res, resveratrol; DMEM-LG, Dulbecco's Minimum Essential Medium-Low Glucose.

releasing resveratrol.¹² However, this is the first report of sustained release of resveratrol from three-dimensional porous solid scaffolds. PCL-RNP could also be synthesized and fabricated into desired dimensions. The therapeutic potential, straightforward synthesis, and fabrication process for PCL-RNP is highly prognostic for its use in grafts for fractures with large bone loss.

Conclusion

In this study, resveratrol was released from scaffolds in a sustained manner. Resveratrol was also amorphized due to its entrapment in nanoparticles, which increased the dissolution of resveratrol. Drug release from PCL-RNP was sustained for 12 days, with a total release of 64%. PCL-RNP was potent in increasing proliferation, induction of alkaline phosphatase, and mineralization. This study emphasizes the use of bioactive small molecules obtained from plant sources for targeting in bone tissue engineering. Prolonged release of these bioactive molecules can potentially overcome the adverse effects elicited by therapeutic delivery of certain indigenous growth factors. To conclude, prolonged release of resveratrol from PCL-RNP is highly desirable in bone tissue engineering because it is osteoconductive and osteoinductive, and promotes osteogenesis.

Acknowledgments

This work was funded by SRM University. We sincerely thank the Nanotechnology Research Centre, SRM University, for providing support with scanning electron microscopy, atomic force microscopy, and X-ray diffraction. The authors express their gratitude to the Dean, School of Bioengineering, SRM University, and the Head of Department of Biotechnology, SRM University, for their support.

Author contributions

The work was hypothesized, designed, and carried out by MSK. All other authors contributed equally with technical and intellectual input.

Disclosure

The authors report no conflicts of interest in this work.

References

- Keating JF, Simpson AH, Robinson CM. The management of fractures with bone loss. *J Bone Joint Surg Br.* 2005;87:142–150.
- Mitchel SE, Keating JF, Robinson CM. The treatment of open femoral fractures with bone loss. *J Bone Joint Surg Br.* 2010;92:1678–1684.
- Thayur RM, Balasundaram R, Manjunath KS, Harshad MS, Dabir CS, Krishnappa N. Outcomes of Ilizarov ring fixation in recalcitrant infected tibial non-unions – a prospective study. *J Trauma Manag Outcomes.* 2008;2:6.
- Nuss KM, von Rechenberg B. Biocompatibility issues with modern implants in bone – a review for clinical orthopedics. *Open Orthop J.* 2008;2:66–78.
- Kim DH, Rhim R, Li L, et al. Prospective study of iliac crest bone graft harvest site pain and morbidity. *Spine J.* 2009;9:886–892.
- Rangasamy J, Krishna PC, Sowmya S, Nair SV, Tetsuya F, Hirroshi T. Chitin scaffolds in tissue engineering. *Int J Mol Sci.* 2011;12:1876–1887.
- Tripathi A, Saravanan S, Pattnaik S, Moorthi A, Partridge NC, Selvamurugan N. Bio-composite scaffolds containing chitosan/nano-hydroxyapatite/nano-copper–zinc for bone tissue engineering. *Int J Biol Macromol.* 2012;50:294–299.
- Eugene JC, Eric LH, Bradley KW. A critical review of recombinant human bone morphogenetic protein-2 trials in spinal surgery: emerging safety concerns and lessons learned. *Spine J.* 2011;11:471–491.
- Scott JH, William LM. Scaffold translation: barriers between concept and clinic. *Tissue Eng Part B Rev.* 2011;17:459–474.
- van Hout WM, Mink van der Molen AB, Breugem CC, Koole R, Van Cann EM. Reconstruction of the alveolar cleft: can growth factor-aided tissue engineering replace autologous bone grafting? A literature review and systematic review of results obtained with bone morphogenetic protein-2. *Clin Oral Investig.* 2011;15:297–303.
- Boraiah S, Paul O, Hawkes D, Wickham M, Lorich DG. Complications of recombinant human BMP-2 for treating complex tibial plateau fractures: a preliminary report. *Clin Orthop Relat Res.* 2009;467:3257–3262.
- Hardeep S, Eric J, Ho-Man K, Lakshmi NS. Fabrication and evaluation of resveratrol loaded polymeric nanofibers. *J Biomater Tissue Eng.* 2012;2:228–235.
- Dai Z, Li Y, Quarles LD, et al. Resveratrol enhances proliferation and osteoblastic differentiation in human mesenchymal stem cells via ER-dependent ERK1/2 activation. *Phytomedicine.* 2007;14:806–814.
- Suzuki A, Guicheux J, Palmer G, et al. Evidence for a role of p38 MAP kinase in expression of alkaline phosphatase during osteoblastic cell differentiation. *Bone.* 2002;30:91–98.
- Mizutani K, Ikeda K, Kawai Y, Yamori Y. Resveratrol stimulates the proliferation and differentiation of osteoblastic MC3T3-E1 cells. *Biochem Biophys Res Commun.* 1998;253:859–863.
- Santos AC, Veiga F, Ribeiro AJ. New delivery systems to improve the bioavailability of resveratrol. *Expert Opin Drug Deliv.* 2011;8:973–990.
- Cottart CH, Nivet-Antoine V, Laguillier-Morizot C, Beaudeau JL. Resveratrol bioavailability and toxicity in humans. *Mol Nutr Food Res.* 2010;54:7–16.
- Merodio M, Arnedo A, Renedo MJ, Irache JM. Ganciclovir-loaded albumin nanoparticles: characterization and in vitro release properties. *Eur J Pharm Sci.* 2001;12:251–259.
- Chuenjitkuntaworn B, Inrung W, Damrongsri D, Mekaapiruk K, Supaphol P, Pavasant P. Polycaprolactone/hydroxyapatite composite scaffolds: preparation, characterization, and in vitro and in vivo biological responses of human primary bone cells. *J Biomed Mater Res A.* 2010;94:241–251.
- Dhanasekaran M, Indumathi S, Lissa RP, Harikrishnan R, Rajkumar JS, Sudarsanam D. A comprehensive study on optimization of proliferation and differentiation potency of bone marrow derived mesenchymal stem cells under prolonged culture condition. *Cytotechnology.* 2013;65:187–197.
- Sittichokechaiwut A, Edwards JH, Scutt AM, Reilly GC. Short bouts of mechanical loading are as effective as dexamethasone at inducing matrix production by human bone marrow mesenchymal stem cells. *Eur Cell Mater.* 2012;20:45–57.
- Gomide V, Zonari AAC, Breyner NM, Goes AM, Pereira MM. ISRN Materials Science. Attachment and proliferation of human-adipose-tissue-derived stem cells on bioactive glass/PVA hybrid scaffolds. Available from: <http://www.hindawi.com/isrn/ms/2011/240864/>. Accessed August 16, 2013.

23. Ahmed SS, Santosh W, Kumar S, Christlet HT. Metabolic profiling of Parkinson's disease: evidence of biomarker from gene expression analysis and rapid neural network detection. *J Biomed Sci.* 2009;16:63.
24. Niranjan R, Koushik C, Saravanan S, Moorthi A, Vairamani M, Selvamurugan N. A novel injectable temperature-sensitive zinc doped chitosan/ β -glycerophosphate hydrogel for bone tissue engineering. *Int J Biol Macromol.* 2013;54:24–29.
25. Mendes JB, Riekes MK, de Oliveira VM, et al. PHBV/PCL microparticles for controlled release of resveratrol: physicochemical characterization, antioxidant potential, and effect on hemolysis of human erythrocytes. *Scientific World Journal.* 2012;2012:542937.

International Journal of Nanomedicine

Publish your work in this journal

The International Journal of Nanomedicine is an international, peer-reviewed journal focusing on the application of nanotechnology in diagnostics, therapeutics, and drug delivery systems throughout the biomedical field. This journal is indexed on PubMed Central, MedLine, CAS, SciSearch®, Current Contents®/Clinical Medicine,

Submit your manuscript here: <http://www.dovepress.com/international-journal-of-nanomedicine-journal>

Journal Citation Reports/Science Edition, EMBase, Scopus and the Elsevier Bibliographic databases. The manuscript management system is completely online and includes a very quick and fair peer-review system, which is all easy to use. Visit <http://www.dovepress.com/testimonials.php> to read real quotes from published authors.

Dovepress